Deep-sea Research Part I-oceanographic Research Papers
November 2015, Volume 105 Pages 186-194
http://dx.doi.org/10.1016/j.dsr.2015.09.005
http://archimer.ifremer.fr/doc/00298/40970/

A comparison of *in situ vs. ex situ* filtration methods on the assessment of dissolved and particulate metals at hydrothermal vents

Cotte Laura [1, 2, 3, *], Waeles Mathieu [1, 2], Pernet-Coudrier Benoît [1, 2], Sarradin Pierre-Marie [3], Cathalot Cécile [4], Riso Ricardo D. [1, 2]

[1] Univ Europeenne Bretagne, Brest, France.
[2] Univ Bretagne Occidentale, Grp Chim Marine, CNRS, IUEM,LEMAR,UMR 6539, F-29280 Plouzane, France.
[3] IFREMER Ctr Brest, Lab Environm Profond LEP DEEP REM, F-29280 Plouzane, France.
[4] IFREMER Ctr Brest, Lab Geochim & Metallogenie LGM GM REM, F-29280 Plouzane, France.

* Corresponding author : Laura Cotte, email address : laura.cotte@univ-brest.fr

Abstract :

The objective of this study was to assess the impact of the filtration method (*in situ vs. ex situ*) on the dissolved/particulate partitioning of 12 elements in hydrothermal samples collected from the Lucky Strike vent field (Mid-Atlantic Ridge; MAR). To do so, dissolved (<0.45 µm) and particulate Mg, Li, Mn, U, V, As, Ba, Fe, Zn, Cd, Pb and Cu were measured using different techniques (HR-ICP-MS, ICP-AES and CCSA). Using *in situ* filtration as a baseline, we showed that *ex situ* filtration (on-board and on shore after freezing) resulted in an underestimation of the dissolved pool, which was counterbalanced by an overestimation of the particulate pool for almost all the elements studied. We also showed that on-board filtration was acceptable for the assessment of dissolved and particulate Mn, Mg, Li and U for which the measurement bias for the dissolved fraction did not exceed 3%. However, *in situ* filtration appeared necessary for the accurate assessment of the dissolved and particulate concentrations of V, As, Fe, Zn, Ba, Cd, Pb and Cu. In the case of Fe, on-board filtration underestimated the dissolved pool by up to 96%. Laboratory filtration (after freezing) resulted in a large bias in the dissolved and particulate concentrations, unambiguously discounting this filtration method for deep-sea chemical speciation studies. We discuss our results in light of the precipitation processes that can potentially affect the accuracy of *ex situ* filtration methods.

Graphical abstract

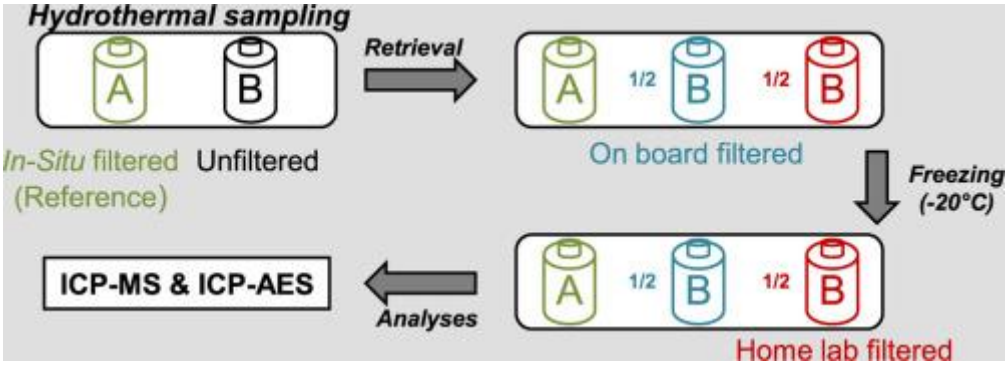

Highlights

► We compared three different filtration methods on hydrothermal samples. ► Dissolved metals are underestimated after post-sampling filtrations. ► On board filtration is suitable for dissolved and particulate Mn, Li, Mg and U. ► *In situ* filtration is essential for V, As, Ba, Fe, Zn, Cd, Pb and Cu. ► Precipitation of sulfides and/or Fe-oxyhydroxide can explain this underestimation.

Keywords : Metal, Hydrothermal vent, Dissolved, Particulate, Filtration method

1. Introduction

Assessing the behavior of trace metals is essential for understanding the link between metal composition and the distribution of deep-sea hydrothermal fauna (Sarradin *et al.* 2008). Some studies have suggested that local biological assemblages are partly controlled by geochemical conditions, including trace metal speciation along the hydrothermal fluid-seawater mixing gradient (Shank *et al.* 1998; Luther *et al.* 2001). The hydrothermal mixing gradient can be schematically split up into three areas: the "anoxic zone" (hot fluid), the "mixing zone", characterized by steep chemical gradients (Johnson *et al.* 1986; Le Bris *et al.* 2003) when hot, reduced hydrothermal fluid mixes with cold, oxidized seawater, and the "oxic zone" (cold seawater).

Substantial efforts have been devoted to understanding the physico-chemical behavior of metal in these different areas. Previous studies assessing the dissolved metal input from hydrothermal vents have focused on the non-buoyant plume (Bennett *et al.* 2008), whereas others have evaluated total dissolvable metal levels in endmember hydrothermal fluids (Charlou *et al.* 2000). Still other studies have considered the chemical composition of particles (Feely *et al.* 1994; German *et al.* 2002) and their kinetics of formation (Rudnicki and Elderfield 1993), focusing on the buoyant and/or the non-buoyant plume of high-temperature black smokers. In the mixing zone, secondary reactions of complexation between dissolved metal and organic metal-binding ligands may influence the chemical speciation of metal, and compete with sulfide precipitation (Sander *et al.* 2007; Toner *et al.* 2009; Yücel *et al.* 2011; Hawkes *et al.* 2013), potentially increasing the dissolved metal flux in the deep ocean (Sander and Koschinsky 2011).

Metal behavior in the mixing zone is still poorly documented despite its significant impact on metal speciation, and data are still lacking in this specific environment (Von Damm *et al.* 1985; Field and Sherrell 2000; Kádár *et al.* 2005; Sander *et al.* 2007; Sarradin *et al.* 2008;

62 Sarradin *et al.* 2009). Data from the mixing zone show substantial variability, likely
63 exacerbated by inappropriate sampling methods and an insufficient number of samples for
64 this study area (Kádár *et al.* 2005). Despite remarkable improvement in the technical means
65 for deep-sea exploration and research over the past 20 years, most scientists perform on-board
66 filtration (typically 0.45 μm) after retrieval of deep-sea samples (Von Damm *et al.* 1985;
67 Sander *et al.* 2007; Bennett *et al.* 2008; Sarradin *et al.* 2009; Yücel *et al.* 2011), despite being
68 aware of the potential alteration of the chemical speciation due to dramatic changes in
69 temperature and pressure and/or chemical equilibrium.
70 Commonly used in surface-water sampling (Gimpel *et al.* 2003), *in situ* filtration can
71 reduce this chemical alteration, potentially caused by precipitation and/or adsorption of some
72 dissolved elements. Obviously, direct *in situ* measurements would provide the best
73 representative data of the fluid chemistry in deep sea environment (Chin *et al.* 1994; Luther *et*
74 *al.* 2001; Vuillemin *et al.* 2009), but only a few trace metals can be measured this way.
75 Hence, there is an urgent need to evaluate the fractionation biases of *in situ* vs. *ex situ*
76 filtration methods and to quantify these biases for various elements.
77 Several specialized samplers have been designed and employed in hydrothermal vents to
78 collect dissolved and particulate samples for *in situ* filtration for various types of analyses
79 (Huber *et al.* 2003; Taylor *et al.* 2006; Preston *et al.* 2011; Ussler *et al.* 2013), including the
80 analysis of dissolved and particulate Fe (Kádár *et al.* 2005; Sarradin *et al.* 2008; Breier *et al.*
81 2009; 2014). However, there have been no comparison of results between *in situ* and *ex situ*
82 sample processing methods.
83 Here, we provide new data from the hydrothermal mixing zone to evaluate the impact of
84 the filtration method (*in situ* vs. *ex situ*) on the dissolved-particulate partitioning of 12
85 elements (Mg, Li, Mn, U, V, As, Ba, Fe, Zn, Cd, Pb and Cu). Kádár *et al.* (2005) also
86 explored this comparative approach, but did not quantitatively assess the particulate phase

because only sweeping electronic microscopy was used to determine the chemical composition of particles. Furthermore, the alteration of the dissolved phase due to *ex situ* filtration was not estimated. Our first objective was to quantify the biases in the assessment of the dissolved and particulate phases potentially induced by *ex situ* filtration methods using *in situ* filtration as a baseline. For each studied metal, we then determined whether it is imperative to filter fluids *in situ* or whether *ex situ* filtration can be acceptable. Our data could guide future studies by indicating the bias introduced by *ex situ* filtration on the chemical speciation of metals.

2. Materials and methods

2.1. Study area

This study was conducted during the MoMARSAT 2012 cruise, on the French oceanographic research vessel Thalassa with the ROV Victor 6000. The cruise focused on deep-sea EMSO-Azores observatory maintenance (SEAMON E/W, Tempo and BOREL buoy) located within the Lucky Strike hydrothermal field, on the Mid-Atlantic Ridge (MAR) (37°17'N) (Colaço *et al.* 2011). In the Lucky Strike field, vent sites are distributed around a lava lake at depths of between 1650 and 1750 m (Fouquet *et al.* 1995). The maximum temperature recorded for the endmember fluid at this location is 324°C (Charlou *et al.* 2000). Water samples were collected on a vent close to the hydrothermal edifice Tour Eiffel (37°17.29'N, 32°16.45'W). Samples were a colorless mixture of mid-temperature fluid (~70°C) and cold seawater, the first part of the mixing likely occurring in subsurface, within the permeable shallow crust. As described in Barreyre *et al.* (2014), this kind of discharge is akin to an intermediate-temperature outflow regime.

2.2. Sampling and filtration

All water samples were collected along the hydrothermal fluid-seawater mixing gradient with the PEPITO sampler implemented on the ROV Victor 6000 (Sarradin *et al.* 2007). This sampling device can sample down to 6000 m depth and was fitted with blood bags (PVC, Baxter Fenwall 2L, sterile/NP-FP, R4R2041). Prior to use, all equipment used for sampling and filtration was rigorously washed three times with diluted hydrochloric acid (pH 2, Suprapur, Merck) and then thoroughly rinsed three times with ultrapure water (Milli-Q element system). Filters were treated as above, but left overnight in diluted hydrochloric acid before the ultrapure water rinse. Each sampling was performed by pumping water into a bag using an acid-cleaned (pH 2, HCl Suprapur, Merck) titanium-Tygon inlet coupled to the ROV temperature probe. Immediately after recovery of the ROV, samples were processed in the chemical lab on board the oceanographic vessel (clean lab, P 100 000; ISO8) and pH was measured on a subsample using a Metrohm pH-meter. Measurements were carried out after daily calibration with NBS buffers (pH 4 and 7) at 25°C. For this study, 17 samples were obtained from two ROV dives (sample list in Table 1). Eight of them were filtered *in situ* (IS samples), whereas the nine others, collected as close as possible to the IS samples, were dedicated to on-board filtration (OB samples) and, after freezing at -20°C, to filtration in the laboratory on shore (LF samples). The OB samples were filtered in a clean room within 2 h of recovery. Laboratory filtration was performed back on shore 18 months later; LF samples were filtered and acidified at pH 2 (HNO_3 65%, Suprapur, Merck) within 2 h of defrosting. Blood bags were homogenized before carrying out the *ex situ* filtration methods. On-board and laboratory filtration methods were performed under gentle vacuum (< 5 psi) using pre-washed mixed cellulose ester filters (0.45 µm, d 47 mm, HATF, Millipore). The filtered volumes varied among samples, ranging from 60 to 1200 mL. Blanks were prepared on board by pumping ultrapure water into a dedicated bag using the acid-cleaned titanium-Tygon inlet.

Filtration blanks were also run in the laboratory. Aliquots and filters were stored in 500 mL Nalgene HDPE bottles and polystyrene petri-slides (Millipore), respectively. HDPE bottles and petri-slides were previously washed with diluted nitric acid (2.5%, Suprapur, Merck) overnight and then thoroughly rinsed with ultrapure water. Petri-slides were dried under a laminar flow hood.

2.3. Analysis of the dissolved fraction

Concentrations of Mn, Li, U, V, As, Ba, Fe and Zn were assessed by high-resolution inductively coupled plasma/mass spectrometry (HR-ICP-MS, Element 2, ThermoFisher, operating at the Pôle Spectrométrie Océan (PSO), Brest). Standards and samples were prepared in 15 mL polypropylene tubes (Elkay), which were pre-cleaned using the same protocol as for the HDPE bottles. The analysis of the dissolved fraction was performed after dilution of the samples in a 2.5% nitric acid solution (dilution factor: 20). Standards of dissolved elements were carried out in a solution of seawater depleted of trace metals (Safe-S, Geotraces reference sample, 2004), and diluted 20-fold in a 2.5% nitric acid solution to match the saline matrix of the dissolved samples. These standards were then spiked with a multi-element solution (AccuStandard; 29 elements; 10 $mg.L^{-1}$). Measurement of Mg concentration was performed using inductively coupled plasma/atomic emission spectrometry (ICP-AES, Ultima 2, Horiba Jobin Yvon, at the PSO in Brest) and specific standards were prepared by diluting decreasing volumes of the Safe-S seawater ([Mg] = 53.0 $mmol.L^{-1}$) in a 2.5% nitric acid solution. Aliquots of acidified seawater (pH2, HCl Suprapur, Merck) were used for the measurement of dissolved Cd, Pb and Cu by constant current stripping analysis (CCSA) with a mercury film electrode (Riso *et al.* 1997). To check the accuracy of the method, certified seawater (CRM-CASS 4) was analyzed. The detection limits were determined by three standard deviations of the blank and summarized in Table 1. In our

160 samples, the dissolved elements were generally well above the limit of detection (LOD) (Mn,
161 Li, U, V, As, Ba, Cd and Pb) except for Cu, Fe and Zn because some samples were collected
162 close to the marine endmember of the gradient and displayed very low concentrations. For
163 ICP-MS measurements, signal drift was assessed and corrected using a standard bracketing
164 approach (one standard every five samples). Blanks were negligible when compared to the
165 dissolved concentrations because they were below the LOD for all the studied elements.
166 Dissolved elements were determined with a precision generally better than 0.5% (Mg), 2.5%
167 (Mn), 4% (Li, U, Ba) or 5% (V). Cd, Pb and Cu levels were assessed with a precision
168 generally better than 4, 3 and 8%, respectively. Due to their low concentrations, Fe, Zn and
169 As had measurement precisions of 18%, 15% and 27%, respectively.
170

171 ## 2.4. Analysis of the particulate fraction

172 Particulate elemental concentrations were assessed by HR-ICP-MS (Element 2,
173 ThermoFisher, operating at the PSO, Brest). The particulate fraction was available after
174 digestion of the entire filter in 4 mL of nitric acid (65%, Suprapur, Merck) and 1 mL of
175 hydrogen peroxide (30%, Suprapur, Merck), by heating to 105°C for 4 h. This acid digestion
176 procedure provides concentrations similar to those of the total digestion method (HNO_3/HF),
177 except for Al (Yafa and Farmer 2006). The use of HF is generally recommended to
178 completely solubilize elements present in resistant minerals, such as aluminosilicates. As
179 hydrothermal particles are mostly made up of soluble sulfide and oxide minerals (Mottl and
180 McConachy 1990; Breier *et al.* 2012) that are relatively well digested with the acid digestion
181 procedure, we did not use HF. Instead, hydrogen peroxide was added to provide better
182 oxidization of particles and to limit the formation of nitrogen dioxide. The evaporation loss
183 during the digestion was checked using the gravimetric method. Certified reference material
184 (PACS-2, NRCC) was used to check digestion efficiency. Concentrations, recoveries and

185 uncertainties obtained for the PACS-2 samples are summarized in Table 2. The percentage of
186 recovery was generally high for As, Fe, Zn, Cd, Pb and Cu (> 70%), indicating an almost
187 complete digestion of particles. The remaining elements showed a lower extraction efficiency
188 (> 50%) because they were probably bound to more resistant minerals such as
189 aluminosilicates. Given that the amount of aluminosilicates was probably limited in our
190 hydrothermal samples, the digestion procedure that we used should be sufficient to correctly
191 solubilize the elements.

Table 2. Results of elemental determination in the certified reference material PACS-2.

	Concentrations ($mg.kg^{-1}$)		
Element	Certified values	Measured values (mean)	% of recovery
Mg	14700 ± 1300	9294 ± 424	63 ± 1
Mn	440 ± 19	227 ± 5	52 ± 1
Li	32.2 ± 2.0	21.9 ± 0.8	68 ± 1
U	3[a]	2.0 ± 0.1	52 ± 1
V	133 ± 5	69 ± 2	52 ± 1
As	26.2 ± 1.5	22.6 ± 1.4	86 ± 1
Fe	40900 ± 600	28865 ± 1663	71 ± 1
Zn	364 ± 23	338 ± 16	93 ± 1
Ba	-[b]	599 ± 37	-[b]
Cd	2.11 ± 0.15	2.10 ± 0.20	99 ± 1
Pb	183 ± 8	172 ± 9	94 ± 1
Cu	310 ± 12	305 ± 33	98 ± 1

[a] Uncertainty not provided
[b] Not available

192 Filter blanks did not significantly affect the measurements of particulate concentrations after
193 digestion, in agreement with the trace metal blanks previously conducted by Planquette and
194 Sherrell (2012) on this filter membrane. The analysis of the particulate fraction was
195 performed after a 1:20 dilution of the digested samples in ultrapure water (final concentration:
196 2.5 % nitric acid). The particulate standards were prepared from the aforementioned multi-
197 element stock solution in a 2.5% nitric acid solution. From filtration to the ICP analysis, the
198 analytical error calculated on PACS-2 was generally better than 10%.
199

3. Results

3.1. Characterization of the sampled mixing zone

The total Mn (Mn_T, equal to the sum of dissolved Mn (Mn_d) and particulate Mn (Mn_p)) concentration was used as the mixing indicator. Total Mn concentrations ranged from 0.02 to 16.08 μM (seawater: ~ 0.5 nM at 1700 m depth, (Yeats *et al.* 1992)). Based on the conservative mixing behavior of Mn (James and Elderfield 1996), the proportion of hydrothermal fluid in the sampled area can be estimated from the concentration of Mn in the hydrothermal endmember fluid at the same site (289 μM; Charlou *et al*. 2000). Hence, our samples covered some of the mixing zone, where the hydrothermal fluid contribution amounted to approximately 0.01% to 6%. Temperature was in the range of 4 to 64°C, with median values below 50°C. The organization of samples according to increasing Mn_T values clearly shows greater variability in temperature in Mn-rich samples (Fig. 1). This higher variability may be due to the greater fraction of hot hydrothermal fluid captured during sampling, possibly enhanced by turbulent mixing with seawater. The dissolved and particulate concentrations measured in all samples (IS, OB and LF) are listed in Table 1. The dissolved/particulate partitioning of all the elements as a function of Mn_T are shown in Fig. 2.

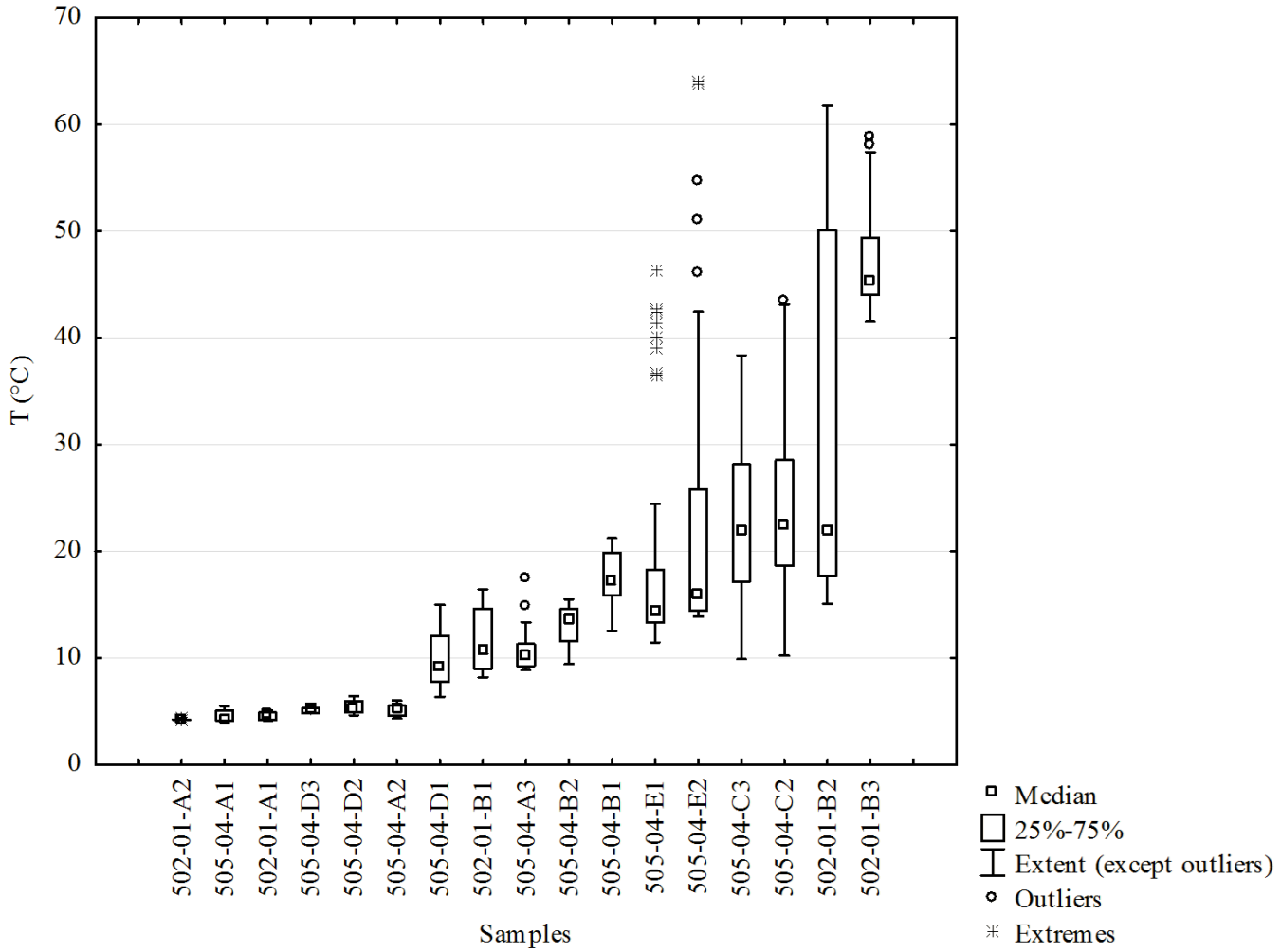

Fig. 1. Ranges of temperature recorded during the 3 minutes of each sampling performed in the study area. Samples are classified by ascending order of Mn_T concentrations. Sample name includes the number of the dive (e.g. 502-01) and the number of the blood bag used for sampling (e.g. A2).

217

218 3.2. **Concentration changes after *ex situ* filtration**

219 Four different groups of elements were discerned according to the predominance of the
220 dissolved or the particulate pools and the degree of physicochemical changes caused by *ex*
221 *situ* filtration. The first group includes Mn, Mg and Li because their dissolved concentrations
222 dominated their particulate concentrations regardless of the filtration method and were the
223 least affected by *ex situ* filtration. U, V and As were grouped together because they showed
224 similar levels of concentrations, with a predominance of the dissolved pool and similar

patterns of changes caused by *ex situ* filtration. The third group clusters Fe, Zn and Ba which generally showed a predominance of the dissolved pool under *in situ* conditions and great variability of their dissolved/particulate partitioning after *ex situ* filtration. The last group includes Cd, Pb and Cu which were mostly found in the particulate phase regardless of the filtration method used. Results obtained for each group are presented in the next four sections.

3.2.1. Mn, Mg and Li

The *in situ* concentrations of dissolved Mn ranged from 0.12 to 14.12 µM. Similar dissolved levels were measured after on-board and laboratory filtration, ranging from 0.02 to 16.08 µM and from 0.12 to 15.45 µM, respectively (Table 1). Particulate concentrations generally remained below 0.02 µM (LOD) when performing *in situ* and on-board filtration, except for the sample 505-04-E2-OB whose particulate Mn was three times greater than the LOD. However, most samples filtered after freezing (6/9) showed particulate concentrations that were 2 to 45 times greater than the LOD (Table 1). The increase in the particulate pool observed should therefore be offset by a decrease in the dissolved concentrations, with the total metal concentrations remaining constant. The underestimation of the dissolved pool was clearly observed when plotting the dissolved/particulate partitioning of Mn, especially after freezing (Fig. 2). Compared with *in situ* conditions in which dissolved Mn accounted for more than 99% of total Mn, the contribution of dissolved Mn was lower after on-board filtration, being decreased by of 0.0 to 3.0%. In samples filtered after freezing, the contribution of dissolved Mn was underestimated by 0.0 to 7.0%.

The *in situ* concentrations of dissolved Mg ranged from 46.7 to 50.6 mM and similar levels were measured with the other filtration methods (Table 1). The *in situ* concentrations of particulate Mg ranged from 21 to 42 µM. Although similar concentrations were found with

249 on-board filtration (26 to 56 µM), particulate concentrations of Mg were clearly higher after
250 laboratory filtration (33 to 205 µM).
251 The *in situ* concentrations of dissolved Li ranged from 24.8 to 41.5 µM (Table 1). As for
252 dissolved Mg, similar levels were found with on-board and laboratory filtration methods,
253 ranging from 26.7 to 46.3 µM and from 26.7 to 45.2 µM, respectively. Particulate
254 concentrations of Li were generally below the LOD except for five samples filtered in the
255 laboratory, which were up to five times greater than the LOD.
256 The dissolved/particulate partitioning of Mg and Li generally changed little with the *ex situ*
257 filtration methods (Fig. 2). Compared to *in situ* conditions in which dissolved Mg and Li
258 accounted for more than 99.9% of total Mg and Li, the contribution of dissolved Mg and Li
259 after on-board filtration was underestimated by only 0.0 to 0.1% and 0.0 to 0.5%,
260 respectively. After freezing, the underestimation increased up to 0.3% and 4.0% for dissolved
261 Mg and Li, respectively.
262

263 **3.2.2. U, V and As**

264 The *in situ* concentrations of dissolved U, V and As ranged from 0.010 to 0.014 µM,
265 0.025 to 0.031 µM and 0.03 to 0.04 µM, respectively (Table 1). Very similar concentrations
266 were obtained after on-board or laboratory filtration, indicating limited differences at first
267 glance.
268 Particulate concentrations of U, V and As were generally below the LOD for *in situ* and on-
269 board filtration methods, with the exception of sample 505-04-E2-OB in which particulate V
270 and As were two and three times greater than the LOD, respectively. However, for most
271 samples filtered in the laboratory (6/9), particulate concentrations of U and V were up to
272 seven and four times greater than the LOD, respectively. A similar trend was observed for

273 particulate As, which was 2 to 14 times greater than the LOD after freezing in three of the
274 nine samples.
275 The dissolved/particulate partitioning of U, V and As also appeared to be affected by *ex situ*
276 filtration (Fig. 2). Compared to *in situ* conditions in which dissolved U, V and As accounted
277 for more than 99%, 96% and 80% of total U, V and As, the contribution of these dissolved
278 elements after on-board filtration was underestimated by 0.0 to 0.4%, 0.0 to 10% and
279 2.0 to 30%, respectively. For samples filtered after freezing, the contribution of dissolved U,
280 V and As was decreased by 0.0 to 30%, 0.0 to 20% and 0.0 to 80%, respectively.
281

282 **3.2.3. Fe, Zn and Ba**

283 The *in situ* concentrations of dissolved Fe ranged from < LOD to 7.46 μM (Table 1). Samples
284 collected at temperatures greater than 10°C showed micromolar concentrations (> 3 μM). In
285 this hotter part of the mixing gradient, the dissolved concentrations were much lower for
286 samples filtered on-board and after freezing. They were generally lower than 1 μM after on-
287 board filtration and below the LOD after freezing.
288 The *in situ* concentrations of dissolved Zn ranged from 0.64 to 1.23 μM (Table 1). As
289 observed for dissolved Fe, concentrations of dissolved Zn measured in Mn-rich samples
290 (Mn_T > ~ 5 μM) dramatically decreased after *ex situ* filtration. Although concentrations near
291 1 μM were measured for samples filtered *in situ*, levels of dissolved Zn found in those filtered
292 on board and after freezing became close to or below the LOD (0.1 μM).
293 The *in situ* concentrations of dissolved Ba ranged from 0.11 to 3.57 μM (Table 1). Although
294 the decrease in the dissolved concentrations was initially less obvious, concentrations were
295 lower after on-board and laboratory filtration (0.06 to 2.36 μM and
296 0.06 to 1.89 μM, respectively).

297 The *in situ* concentrations of particulate Fe, Zn and Ba ranged from < LOD to 1.62 μM,
298 < LOD to 3.42 μM and < LOD to 1.39 μM, respectively. Due to the decrease in the dissolved
299 fraction, the particulate concentrations increased in *ex situ* filtration, especially for Fe and Zn.
300 Particulate concentrations of Fe and Zn after on-board filtration ranged from
301 < LOD to 11.9 μM (mean: 2.6 μM) and from < LOD to 40.1 μM (mean: 5.8 μM),
302 respectively. For samples filtered after freezing, concentration ranges were wider because
303 particulate Fe and Zn ranged from < LOD to 92.2 μM (mean: 15.9 μM) and from
304 0.14 to 140 μM (mean: 16.6 μM), respectively. The increase in particulate Ba was restricted:
305 concentrations after on-board and laboratory filtration ranged from < LOD to 2.02 μM and
306 from < LOD to 4.94 μM, respectively.
307 These changes in dissolved and particulate Ba, Fe and Zn after *ex situ* filtration were also
308 clearly observed in Fig. 2. Compared with *in situ* conditions, dissolved Fe, Zn and Ba after
309 on-board filtration were underestimated in the range of 2.0 to 96%, 1.0 to 99% and
310 0.0 to 34%, respectively. After freezing, dissolved Fe, Zn and Ba decreased by 94 to 100%,
311 20 to 100% and 2.0 to 70%, respectively.
312

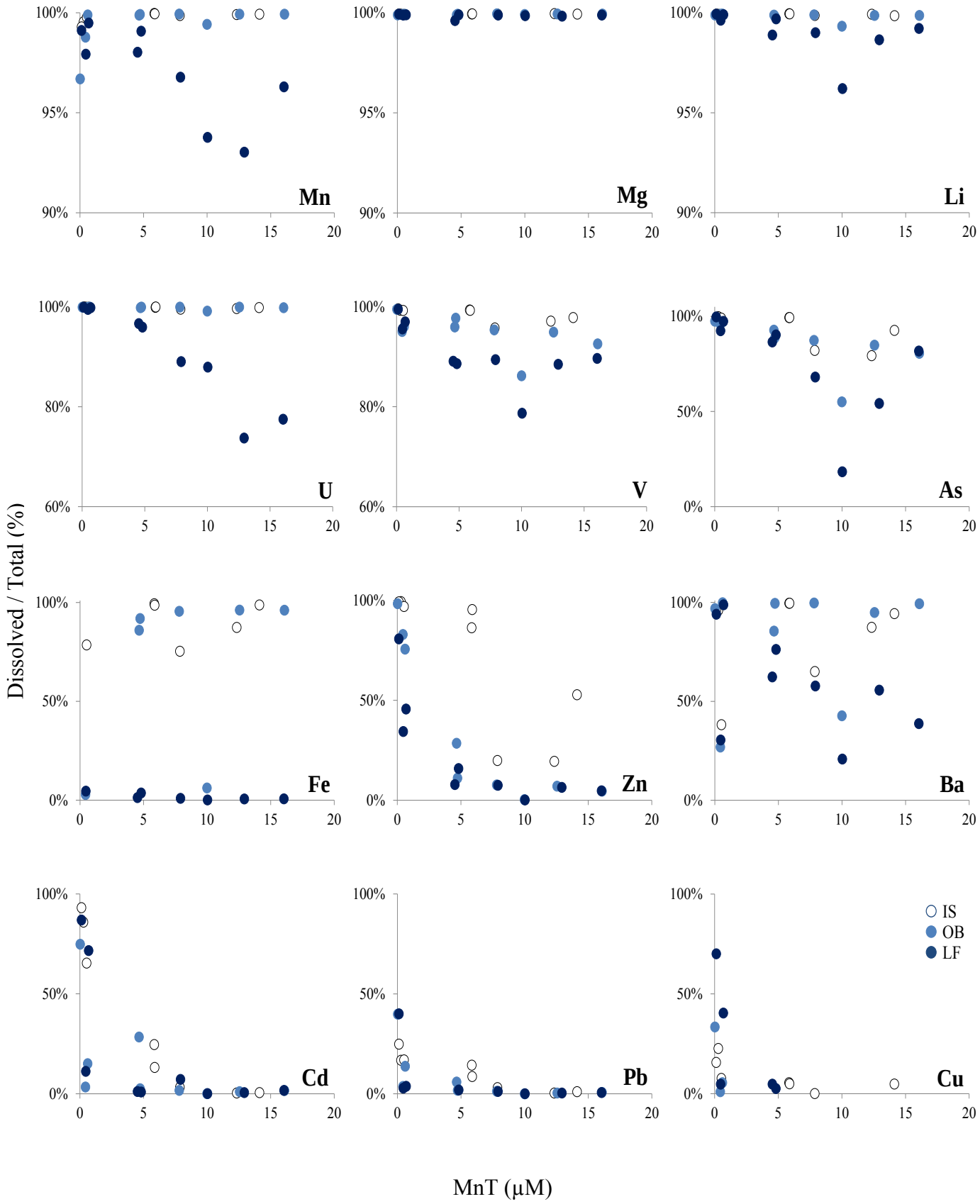

Fig. 2. Contribution of the dissolved phase (%) to total metal concentrations as a function of Mn_T (µM). Dots represent the dissolved phase: white circles refer to *in situ* filtration (IS), blue circles to on-board filtration (OB) and dark blue circles to laboratory filtration, after freezing (LF). The scale for the contribution of dissolved Mn, Li, Mg, U and V was magnified to better show effects/differences potentially induced by *ex situ* filtration.

3.2.4. Cd, Pb and Cu

The *in situ* concentrations of dissolved and particulate Cd, Pb and Cu were observed at subnanomolar to nanomolar levels. The *in situ* concentrations and those measured after *ex situ* filtration were generally close to the LOD, indicating that modifications in the dissolved and particulate phases were difficult to assess. The only exception was for concentrations of dissolved Pb, for which a significant decrease of almost one order of magnitude was observed for on-board and laboratory filtration (Table 1).

Our data also indicated that the dissolved/particulate partitioning changed with *ex situ* filtration. For samples filtered *in situ*, the contribution of the dissolved fraction tended to increase with the dilution of the hydrothermal fluid, reaching a maximum level at the lowest Mn_T levels (Fig. 2). The increase ranged from few percentage points at Mn_T = 14 µM to ~ 90%, ~ 25% and ~ 20% at Mn_T = 0.12 µM for Cd, Pb and Cu, respectively. This pattern was weaker for *ex situ* filtration, which generally caused an underestimation of the contribution of the dissolved pool in the coldest part of the gradient.

4. Discussion

Our results highlighted an underestimation of dissolved metal concentrations accompanied by an overestimation of the particulate phase when *ex situ* filtration is performed. The modifications of the dissolved and particulate pools varied according to the element. Below, we inventory the elements that can be properly assessed using *ex situ* — shipboard or laboratory — filtration methods. We then discuss the chemical processes that may explain the observed biases.

4.1. Which elements require *in situ* filtration?

Of the three filtration methods performed, the *in situ* method is of course the best one for obtaining representative data on metal chemistry in the deep-sea environment. The degree of sensitivity of the dissolved and particulate pools of each sample after *ex situ* filtration was therefore assessed using the *in situ* filtration as a baseline. Many laboratories perform on-board filtration to assess metal concentrations, requiring a study of its suitability for properly characterizing the dissolved and particulate phases. Although rarely used, filtration after freezing was also interesting to investigate because it can serve as an extreme example of the bias caused by freezing and delayed filtration.

In samples filtered on board, our results show that dissolved Mn, Mg, Li and U were the least affected of all the elements studied: the underestimation of the dissolved phase did not exceed 3%. Hence, dissolved concentrations of Mn, Mg, Li, and U were not significantly affected by the on-board filtration method, which thus appears suitable for properly characterizing the dissolved pool of these four elements. Particulate concentrations after on-board filtration obtained for Mg were generally similar to the *in situ* concentrations and generally remained below the LOD for Mn, Li and U (Table 1). This pattern suggests that modifications of the particulate pool for these elements are only slight, although more precise quantification of the particulate concentrations is required for confirmation.

For V and As, limited changes occurred after on-board filtration, but our results showed that the contribution of the dissolved concentrations can decrease by 10% and 30%, respectively. The observed underestimation was mainly driven by the single, aforementioned particle-rich sample (505-04-E2-OB), explaining both maximum percentages observed. Without the influence of this outlier sample, dissolved V and As after the on-board filtration would be underestimated by up to ~ 5% and ~ 15%, respectively (Fig. 2). Given these relatively high percentages, the *in situ* filtration method is preferable for these two elements.

365 The most affected elements were Fe, Zn, and Ba (Fig. 2). For some samples filtered on board,
366 the dissolved phase had mostly converted into particles (e.g. Zn), which greatly distorted the
367 initial dissolved/particulate partitioning of these elements. As mentioned above for V and As,
368 the underestimation of dissolved Fe and Ba observed can be attributed to the outlier sample
369 505-04-E2-OB. However, the percentages of underestimation still remain high even without
370 its influence, with underestimation ranging from a few percent to ~ 30% and ~ 96%,
371 respectively (Fig. 2). Consequently, the routine use of the *in situ* filtration method is strongly
372 recommended for the accurate quantification of the dissolved and particulate phases of these
373 three elements.
374 Regarding dissolved and particulate Cd, Pb and Cu, results are less conclusive although they
375 suggest that shipboard filtration underestimates the dissolved phase (Table 1, Fig. 2). This
376 underestimation was clear for dissolved Pb concentrations, which were significantly lower
377 compared with *in situ* filtered samples. The dissolved/particulate partitioning of Cd and Pb
378 also showed that the contribution of the dissolved pool after on-board filtration was lower in
379 the cold part of the mixing gradient (Fig. 2). As a precaution, *in situ* filtration should therefore
380 be preferred for proper assessment of these three elements.
381 Filtration after freezing causes a large bias in the dissolved and particulate concentrations for
382 all the elements studied (Fig. 2). Therefore, this filtration method is definitely not
383 recommended.
384

385 ## 4.2. On the processes occurring in *ex situ* filtration

386 As the decrease in the dissolved fraction was generally counterbalanced by an increase of the
387 particulate fraction, most of the changes occurring during *ex situ* filtration can be attributed to
388 various precipitation/scavenging processes. Unfortunately, adsorption of the elements onto the
389 blood bags or the bottle walls cannot be fully excluded. This type of adsorption has been

390 demonstrated for several elements in natural waters (Truitt and Weber 1979). However, the
391 relatively low pH of our samples, combined with the rapidity with which the on-board
392 filtration was carried out after retrieval (< 2 h) and the storage of filtered samples in acid-
393 cleaned PVC bags or HDPE bottles, should limit losses due to adsorption (Batley and Gardner
394 1977).

395 To better understand precipitation/scavenging processes, correlations between all
396 particulate elements were investigated and are summarized in Table 3. The statistically
397 significant correlations (p-value < 0.05) discriminate two main groups of highly correlated
398 elements. The first one groups particulate Mn, Li, U, V, As, Ba and Fe, whereas the second
399 one is composed of Cd, Pb, Cu and Zn. Other sub-groups were also involved but correlations,
400 though statistically significant, were less pronounced (Table 3). Here, we only focus on the
401 two aforementioned groups.

402 The high positive correlations between particulate Mn, Li, U, V, As, Ba and Fe suggest
403 that dissolved Mn, Li, U, V, As and Ba may have been primarily scavenged by Fe-oxide
404 particles during the *ex situ* filtration process. Dissolved Fe levels from hydrothermal vents can
405 be affected by two chemical precipitation processes: entrapment by sulfide particles and
406 formation of Fe-oxyhydroxides (Mottl and McConachy 1990; Rudnicki and Elderfield 1993).
407 The co-precipitation of Fe(II) in polymetallic sulfide phases occurs immediately upon fluid
408 discharge, whereas Fe-oxide particles are formed later in more oxidizing conditions (Rudnicki
409 and Elderfield 1993). Each precipitation process has been suggested to account for 80-90%
410 and 10-20% of dissolved Fe removal, respectively (German *et al.* 2002). Once formed, small
411 Fe-rich sulfide particles are exported in the buoyant and neutrally buoyant plume (Yücel *et al.*
412 2011; Breier *et al.* 2012), showing that reduced and oxidized particles can coexist in the
413 diluted plume. This two-stage precipitation process occurs in hot focused black smokers
414 where sulfides are abundant. However, our samples come from an intermediate-temperature

415 vent that emits a colorless and translucent mixture of hot hydrothermal fluid (~ 70°C) and
416 cold seawater. Given that the first part of mixing probably occurs in the shallow crust, most of
417 the sulfides would have precipitated in the subsurface. The large underestimations of
418 dissolved Fe observed throughout the *ex situ* filtration process should therefore mainly come
419 from oxidative precipitation such as Fe-oxyhydroxide formation. Our samples may thus be
420 made up of pre-existing Fe-oxide particles that formed before sampling, but also of newly
421 formed Fe-oxides that may have precipitated post-sampling.
422 Away from vent sources, dissolved Mn is commonly known to undergo slow scavenging
423 processes by suspended particles (Cowen *et al.* 1990; Feely *et al.* 1994), which are enhanced
424 by Mn(II)-oxidizing bacteria (Mandernack and Tebo 1993). German *et al*. (1991) also
425 observed a correlation ($r^2 = 0.610$) between particulate Mn and Fe in the diluted plume,
426 suggesting progressive scavenging of dissolved Mn onto Fe-rich particulate phases, which are
427 mainly Fe-oxyhydroxide particles. Dissolved Ba has been suggested to undergone similar
428 scavenging processes as those reported for dissolved Mn (Feely *et al.* 1994). This element
429 could therefore be scavenged by Fe-oxyhydroxide particles.
430 Other precipitation processes not revealed by the correlations may explain the modifications
431 of the dissolved and particulate pool observed for Mn and Ba. Regarding Mn, precipitation of
432 MnO_2 may occur in our samples, assuming that oxygen levels increased slightly during *ex situ*
433 filtration. In the case of Ba, precipitation of barite may occur because our samples are a
434 mixture of fluid and entrained sulfate-rich seawater (Charlou *et al.* 2000).
435 As observed for Mn and Ba, scavenging processes from seawater enhanced by physico-
436 chemical changes (T, p, O_2) during retrieval and freezing/defrosting of samples may explain
437 the changes in phase distribution observed for U, V and As. Previous studies have highlighted
438 pronounced linear correlations of particulate U, V and As with particulate Fe, suggesting that

439 Fe-oxyhydroxide particles rapidly scavenge dissolved U, V and As from the seawater
440 (German *et al.* 1991; Feely *et al.* 1994; Kadko *et al.* 1994; Breier *et al.* 2012).

441 The high correlations between particulate Zn, Cd, Pb, and Cu suggest that Cd, Pb and Cu
442 precipitated in a wurtzite or sphalerite phase. This supposition is supported by previous
443 reports of the formation of Cd, Pb, Cu and Zn precipitates in sulfide minerals, suggesting a
444 co-precipitation of dissolved Cd, Pb, Cu and Zn directly from vent fluids (Trocine and Trefry
445 1988; German *et al.* 1991; Sarradin *et al.* 2008; Breier *et al.* 2012).

446 In addition, nanoparticle aggregation mechanisms, such as flocculation, may explain the
447 observed changes in the dissolved and particulate pools. Recent studies on particle
448 morphology all observed a natural aggregation of particles in their *in situ* hydrothermal
449 samples (Breier *et al.* 2012; Toner *et al.* 2012). If there is a limited artefact of *in situ* filtration
450 on the aggregation mechanism (Breier *et al.* 2012), *ex situ* filtration may enhance this natural
451 process, potentially explaining the overestimation of the particulate pool. A characterization
452 of the nature of particles is required to confirm these hypotheses on these potentially
453 occurring precipitation processes.

454

455

456

5. Conclusion

We assessed the impact of the filtration method (*in situ* vs. *ex situ*) on the dissolved/particulate partitioning of 12 elements. Depending on the metal considered, a decrease in dissolved metal concentrations, counterbalanced by an increase in particle levels, occur in *ex situ* filtration. Four groups of elements showing similar patterns of changes in their dissolved and particulate concentrations were described: 1) Mn, Mg and Li; 2) U, V and As; 3) Fe, Zn and Ba; 4) Cd, Pb and Cu. On-board filtration appears sufficient to properly assess dissolved and particulate Mn, Mg, Li, and U with very limited changes in the concentrations compared with those measured after *in situ* filtration. However, on-board filtration is not suitable for accurately measuring the dissolved and particulate concentrations of V, As, Fe, Zn, Ba, Cd, Pb and Cu, for which there were large underestimations of the particulate pool. *In situ* filtration should therefore be used routinely to accurately characterize the dissolved and particulate phases of these elements. Laboratory filtration is definitely not recommended because it causes large biases in concentrations. Scavenging of metals by Fe-oxyhydroxide particles may explain the changes observed for Mn, U, V, As and Ba. Particulate Cd, Pb, Cu and Zn were highly correlated suggesting co-precipitation of these metals in a wurtzite or sphalerite phase.

Overall, our results clearly improve our understanding of the impact caused by *ex situ* filtration on the dissolved and particulate distribution of metals. Therefore, all chemical speciation data based on shipboard filtration already described in the literature may not fully represent the original species found in the deep-sea environment. This bias may have relevant implications for the computation of hydrothermal metal export fluxes to the deep ocean.

Acknowledgments

We would like to thank Mathilde Cannat, chief scientist of the MoMARSAT 2012 cruise, the R/V Thalassa crew and the Victor 6000 ROV pilots for their assistance and constant support. We are grateful to Virginie Tanguy for her excellent work during this sampling campaign. We also acknowledge Claire Bassoulet, Céline Liorzou and Marie-Laure Rouget for their helpful assistance in instrumental analyses. This work was carried out with the financial support of Labex Mer (Ironman project, axe 3, IUEM, Brest). It was also supported by a doctoral grant from MENRT and IFREMER. We are grateful to Dr. Carolyn Engel-Gautier (Chrysalide, Finistere, France) for her linguistic editing. Finally, we wish to acknowledge three anonymous reviewers for their helpful and constructive comments.

Table 1. Dissolved and particulate concentrations measured in the 26 samples with their associated limits of detection (LOD). D refers to dissolved concentration (<0.45µm), P to particulate concentration. IS: *in situ* filtration, OB: on-board filtration (after retrieval) and LF: laboratory filtration (after freezing). Sample name is composed of the number of the dive (e.g. 502-01) and the number of the blood bag used for sampling (e.g. A1). Samples are classified according to the filtration method used (gray-scale) and by ascending Mn_T concentration. *Dissolved Cd, Pb and Cu were at nanomolar levels.

Sample	T°C	pH	Mn		Mg		Li		U		V		As		Fe		Zn		Ba		Cd*		Pb*		Cu*	
			µM		mM	µM	µM		µM		µM		µM		µM		µM		µM		nM		nM		nM	
			D	P	D	P	D	P	D	P	D	P	D	P	D	P	D	P	D	P	D	P	D	P	D	P
		LOD	**0.004**	**0.02**	**0.02**	**3**	**0.06**	**0.3**	**0.0001**	**0.0004**	**0.003**	**0.002**	**0.001**	**0.009**	**0.2**	**0.05**	**0.1**	**0.04**	**0.01**	**0.005**	**0.01**	**0.5**	**0.01**	**2**	**0.7**	**10**
505-04-A1-IS	4.6	7.6	0.12	< LOD	50.6	32	25.3	< LOD	0.014	< LOD	0.031	< LOD	0.03	< LOD	< LOD	< LOD	0.66	< LOD	0.11	< LOD	0.20	< LOD	< LOD	< LOD	0.8	< LOD
502-01-A1-IS	4.6	7.5	0.28	< LOD	49.4	37	24.8	< LOD	0.013	< LOD	0.028	< LOD	0.04	< LOD	< LOD	0.05	1.04	< LOD	0.16	0.01	0.13	< LOD	0.02	< LOD	2.0	< LOD
505-04-D2-IS	5.4	7.3	0.53	< LOD	48.6	42	25.4	< LOD	0.014	< LOD	0.028	< LOD	0.03	< LOD	0.23	0.06	1.23	< LOD	0.28	0.44	0.08	< LOD	0.05	< LOD	< LOD	< LOD
505-04-A3-IS	11	6.2	5.85	< LOD	49.4	29	31.6	< LOD	0.013	< LOD	0.028	< LOD	0.04	< LOD	3.77	< LOD	0.64	0.10	2.03	0.01	0.20	0.6	0.29	< LOD	< LOD	< LOD
505-04-B2-IS	13	6.1	5.88	< LOD	48.7	27	31.4	< LOD	0.013	< LOD	0.028	< LOD	0.04	< LOD	3.90	0.06	0.64	< LOD	2.02	0.01	0.05	< LOD	0.12	< LOD	0.8	16
505-04-E1-IS	19	6.1	7.86	< LOD	46.9	30	33.5	< LOD	0.012	< LOD	0.029	< LOD	0.04	< LOD	4.93	1.62	0.85	3.42	2.59	1.39	0.23	6.9	0.28	9	< LOD	111
505-04-C3-IS	23	5.7	12.33	< LOD	46.7	21	38.2	< LOD	0.010	< LOD	0.025	< LOD	0.03	< LOD	4.43	0.64	0.69	2.85	2.66	0.38	0.02	4.9	0.03	10	< LOD	48
502-01-B2-IS	34	4.4	14.12	< LOD	47.1	31	41.5	< LOD	0.010	< LOD	0.028	< LOD	0.04	< LOD	7.46	0.10	0.77	0.69	3.57	0.21	0.02	3.0	0.07	7	2.1	43
502-01-A2-OB	4.2		0.02	< LOD	50.3	56	26.7	< LOD	0.014	< LOD	0.031	< LOD	0.03	< LOD	< LOD	< LOD	0.75	< LOD	0.06	< LOD	0.18	< LOD	0.03	< LOD	1.7	< LOD
505-04-D3-OB	5.1	7.2	0.44	< LOD	50.8	40	26.9	< LOD	0.015	< LOD	0.029	< LOD	0.03	< LOD	< LOD	0.39	1.31	0.27	0.21	0.58	0.01	< LOD	0.02	< LOD	< LOD	12
505-04-A2-OB	5.1	7.3	0.61	< LOD	51.3	41	27.8	< LOD	0.014	< LOD	0.031	< LOD	0.04	< LOD	< LOD	0.31	0.31	0.10	0.28	< LOD	0.03	< LOD	0.02	< LOD	< LOD	< LOD
505-04-D1-OB	10	6.3	4.65	< LOD	52.0	56	32.0	< LOD	0.014	< LOD	0.027	< LOD	0.03	< LOD	2.69	0.44	0.11	0.28	1.66	0.28	0.13	< LOD	0.05	< LOD	< LOD	26
502-01-B1-OB	12	6.3	4.73	< LOD	50.7	36	31.8	< LOD	0.013	< LOD	0.024	< LOD	0.03	< LOD	0.40	< LOD	< LOD	0.84	1.26	0.01	0.02	0.8	0.02	< LOD	< LOD	12
505-04-B1-OB	17	6.2	7.81	< LOD	49.0	26	34.8	< LOD	0.012	< LOD	0.022	< LOD	0.04	< LOD	0.70	< LOD	< LOD	1.26	1.44	< LOD	0.02	1.0	0.02	< LOD	< LOD	14
505-04-E2-OB	22	5.9	9.94	0.06	50.1	42	39.6	< LOD	0.012	< LOD	0.023	0.004	0.04	0.03	0.77	11.9	< LOD	40.1	1.50	2.02	< LOD	77	< LOD	36	< LOD	701
505-04-C2-OB	24	5.7	12.55	< LOD	48.4	31	40.7	< LOD	0.011	< LOD	0.024	< LOD	0.03	< LOD	0.99	< LOD	< LOD	1.38	1.40	0.08	0.02	1.7	< LOD	2	< LOD	< LOD
502-01-B3-OB	47	5.7	16.08	< LOD	47.9	32	46.3	< LOD	0.010	< LOD	0.021	< LOD	0.03	< LOD	1.88	0.08	< LOD	2.22	2.36	0.02	0.03	1.9	0.03	4	< LOD	22
502-01-A2-LF	4.2		0.12	< LOD	50.3	33	26.7	< LOD	0.014	< LOD	0.032	< LOD	0.03	< LOD	< LOD	< LOD	0.61	0.14	0.06	< LOD	0.18	< LOD	0.03	< LOD	2.6	< LOD
505-04-D3-LF	5.1		0.46	< LOD	50.8	58	27.0	< LOD	0.014	< LOD	0.033	< LOD	0.03	< LOD	< LOD	0.39	0.81	1.54	0.21	0.49	0.05	< LOD	0.02	< LOD	0.8	15
505-04-A2-LF	5.1		0.69	< LOD	51.3	53	27.8	< LOD	0.014	< LOD	0.030	< LOD	0.03	< LOD	< LOD	0.26	0.16	0.20	0.28	< LOD	0.16	< LOD	< LOD	< LOD	2.2	< LOD
505-04-D1-LF	10		4.44	0.09	52.0	206	32.2	0.4	0.013	0.0005	0.028	0.003	0.04	< LOD	< LOD	3.54	< LOD	1.24	1.38	0.83	0.02	1.6	< LOD	2	4.6	94
502-01-B1-LF	12		4.78	0.04	50.7	53	30.8	< LOD	0.013	0.0006	0.026	0.003	0.03	< LOD	< LOD	3.97	0.25	1.35	1.46	0.45	0.01	1.4	0.12	6	< LOD	24
505-04-B1-LF	17		7.66	0.26	49.0	58	35.1	0.4	0.011	0.0013	0.029	0.003	0.04	0.02	< LOD	5.37	< LOD	1.30	1.52	1.11	0.10	1.3	0.02	2	< LOD	24
505-04-E2-LF	22		9.41	0.63	50.1	74	36.6	1.4	0.011	0.0015	0.028	0.008	0.03	0.13	< LOD	92.2	< LOD	140	1.30	4.94	0.01	261	< LOD	111	< LOD	2330
505-04-C2-LF	24		12.03	0.90	48.4	84	41.9	0.6	0.008	0.0029	0.028	0.004	0.03	0.03	< LOD	9.20	< LOD	1.53	1.89	1.51	0.01	1.7	< LOD	3	< LOD	17
502-01-B3-LF	47		15.45	0.59	47.9	55	45.2	0.4	0.009	0.0025	0.028	0.003	0.04	< LOD	< LOD	12.0	< LOD	2.12	1.78	2.82	0.05	2.8	0.02	4	< LOD	27

Table 3. Correlation coefficients between particulate concentrations of all the elements studied (12 variables analyzed). All samples were included except 505-04-E2 whose large concentration in particles would introduce substantial bias. Statistically significant correlations are shown in gray (p-value < 0.05). There are two main groups of highly correlated elements: 1) particulate Mn, Li, U, V, As, Ba and Fe; 2) Cd, Pb, Cu and Zn. There are also four smaller groups with less pronounced correlations, though statistically significant: 1) particulate Mg, Li, V and Cu; 2) Ba, Zn, Cd and Cu; 3) As, Zn and Cd; 4) V and Zn.

	Mn_P	Mg_P	Li_P	U_P	V_P	As_P	Fe_P	Zn_P	Ba_P	Cd_P	Pb_P	Cu_P
Mn_P		0.28	0.89	0.98	0.67	0.80	0.90	0.29	0.76	0.16	0.09	0.04
Mg_P	0.28		0.61	0.31	0.58	0.25	0.37	0.04	0.30	-0.05	-0.10	0.44
Li_P	0.89	0.61		0.91	0.84	0.83	0.87	0.33	0.73	0.16	0.10	0.26
U_P	0.98	0.31	0.91		0.75	0.78	0.96	0.31	0.82	0.17	0.12	0.06
V_P	0.67	0.58	0.84	0.75		0.71	0.81	0.47	0.69	0.24	0.26	0.35
As_P	0.80	0.25	0.83	0.78	0.71		0.70	0.59	0.60	0.43	0.38	0.29
Fe_P	0.90	0.37	0.87	0.96	0.81	0.70		0.39	0.90	0.26	0.22	0.20
Zn_P	0.29	0.04	0.33	0.31	0.47	0.59	0.39		0.55	0.87	0.81	0.67
Ba_P	0.76	0.30	0.73	0.82	0.69	0.60	0.90	0.55		0.48	0.34	0.42
Cd_P	0.16	-0.05	0.16	0.17	0.24	0.43	0.26	0.87	0.48		0.92	0.80
Pb_P	0.09	-0.10	0.10	0.12	0.26	0.38	0.22	0.81	0.34	0.92		0.69
Cu_P	0.04	0.44	0.26	0.06	0.35	0.29	0.20	0.67	0.42	0.80	0.69	

References

Barreyre T., Escartín J., Sohn R.A., Cannat M., Ballu V. and Crawford W.C. (2014). "Temporal variability and tidal modulation of hydrothermal exit-fluid temperatures at the Lucky Strike deep-sea vent field, Mid-Atlantic Ridge." *Journal of Geophysical Research* **119**(4): 2543-2566.

Batley G.E. and Gardner D. (1977). "Sampling and storage of natural waters for trace metal analysis." *Water Research* **11**(9): 745-756.

Bennett S.A., Achterberg E.P., Connelly D.P., Statham P.J., Fones G.R. and German C.R. (2008). "The distribution and stabilisation of dissolved Fe in deep-sea hydrothermal plumes." *Earth and Planetary Science Letters* **270**(3–4): 157-167.

Breier J.A., Rauch C.G., McCartney K., Toner B.M., Fakra S.C., White S.N. and German C.R. (2009). "A suspended-particle rosette multi-sampler for discrete biogeochemical sampling in low-particle-density waters." *Deep Sea Research I* **56**(9): 1579-1589.

Breier J.A., Toner B.M., Fakra S.C., Marcus M.A., White S.N., Thurnherr A.M. and German C.R. (2012). "Sulfur, sulfides, oxides and organic matter aggregated in submarine hydrothermal plumes at 9°50′N East Pacific Rise." *Geochimica et Cosmochimica Acta* **88**(0): 216-236.

Breier J.A., Sheik C.S., Gomez-Ibanez D., Sayre-McCord R.T., Sanger R., Rauch C., Coleman M., Bennett S.A., Cron B.R., Li M., German C.R., Toner B.M. and Dick G.J. (2014). "A large volume particulate and water multi-sampler with *in situ* preservation for microbial and biogeochemical studies." *Deep Sea Research I* **94**(0): 195-206.

Charlou J.L., Donval J.P., Douville E., Jean-Baptiste P., Radford-Knoery J., Fouquet Y., Dapoigny A. and Stievenard M. (2000). "Compared geochemical signatures and the evolution of Menez Gwen (37°50′N) and Lucky Strike (37°17′N) hydrothermal fluids, south of the Azores Triple Junction on the Mid-Atlantic Ridge." *Chemical Geology* **171**(1–2): 49-75.

Chin C.S., Coale K.H., Elrod V.A., Johnson K.S., Massoth G.J. and Baker E.T. (1994). "In situ observations of dissolved iron and manganese in hydrothermal vent plumes, Juan de Fuca Ridge." *Journal of Geophysical Research* **99**(B3): 4969-4984.

Colaço A., Blandin J., Cannat M., Carval T., Chavagnac V., Connelly D., Fabian M., Ghiron S., Goslin J., Miranda J.M., Reverdin G., Sarrazin J., Waldmann C. and Sarradin P.M. (2011). "MoMAR-D: a technological challenge to monitor the dynamics of the Lucky Strike vent ecosystem." *ICES Journal of Marine Science* **68**(2): 416-424.

Cowen J.P., Massoth G.J. and Feely R.A. (1990). "Scavenging rates of dissolved manganese in a hydrothermal vent plume." *Deep Sea Research A* **37**(10): 1619-1637.

Feely R.A., Gendron J.F., Baker E.T. and Lebon G.T. (1994). "Hydrothermal plumes along the East Pacific Rise, 8°40′ to 11°50′N: Particle distribution and composition." *Earth and Planetary Science Letters* **128**(1–2): 19-36.

Field M.P. and Sherrell R.M. (2000). "Dissolved and particulate Fe in a hydrothermal plume at 9°45′N, East Pacific Rise: Slow Fe (II) oxidation kinetics in Pacific plumes." *Geochimica et Cosmochimica Acta* **64**(4): 619-628.

Fouquet Y., Ondreas H., Charlou J.L., Donval J.P., Radford-Knoery J., Costa I., Lourenco N. and Tivey M.K. (1995). "Atlantic lava lakes and hot vents." *Nature* **377**(6546): 201-201.

German C.R., Campbell A.C. and Edmond J.M. (1991). "Hydrothermal scavenging at the Mid-Atlantic Ridge: Modification of trace element dissolved fluxes." *Earth and Planetary Science Letters* **107**(1): 101-114.

German C.R., Colley S., Palmer M.R., Khripounoff A. and Klinkhammer G.P. (2002). "Hydrothermal plume-particle fluxes at 13°N on the East Pacific Rise." *Deep Sea Research I* **49**(11): 1921-1940.

Gimpel J., Zhang H., Davison W. and Edwards A.C. (2003). "In Situ Trace Metal Speciation in Lake Surface Waters Using DGT, Dialysis, and Filtration." *Environmental Science & Technology* **37**(1): 138-146.

Hawkes J.A., Gledhill M., Connelly D.P. and Achterberg E.P. (2013). "Characterisation of iron binding ligands in seawater by reverse titration." *Analytica Chimica Acta* **766**: 53-60.

Huber J.A., Butterfield D.A. and Baross J.A. (2003). "Bacterial diversity in a subseafloor habitat following a deep-sea volcanic eruption." *FEMS Microbiology Ecology* **43**(3): 393-409.

James R.H. and Elderfield H. (1996). "Dissolved and particulate trace metals in hydrothermal plumes at the Mid-Atlantic Ridge." *Geophysical Research Letters* **23**(23): 3499-3502.

Johnson K.S., Beehler C.L., Sakamoto-Arnold C.M. and Childress J.J. (1986). "In situ Measurements of Chemical Distributions in a Deep-Sea Hydrothermal Vent Field." *Science* **231**(4742): 1139-1141.

Kádár E., Costa V., Martins I., Santos R.S. and Powell J.J. (2005). "Enrichment in trace metals (Al, Mn, Co, Cu, Mo, Cd, Fe, Zn, Pb and Hg) of macro-invertebrate habitats at hydrothermal vents along the Mid-Atlantic Ridge." *Hydrobiologia* **548**(1): 191-205.

Kadko D., Feely R. and Massoth G. (1994). "Scavenging of ^{234}Th and phosphorus removal from the hydrothermal effluent plume over the North Cleft segment of the Juan de Fuca Ridge." *Journal of Geophysical Research* **99**(B3): 5017-5024.

Le Bris N., Sarradin P.-M. and Caprais J.-C. (2003). "Contrasted sulphide chemistries in the environment of 13°N EPR vent fauna." *Deep Sea Research I* **50**(6): 737-747.

Luther G.W., Rozan T.F., Taillefert M., Nuzzio D.B., Di Meo C., Shank T.M., Lutz R.A. and Cary S.C. (2001). "Chemical speciation drives hydrothermal vent ecology." *Nature* **410**(6830): 813-816.

Mandernack K.W. and Tebo B.M. (1993). "Manganese scavenging and oxidation at hydrothermal vents and in vent plumes." *Geochimica et Cosmochimica Acta* **57**(16): 3907-3923.

Mottl M.J. and McConachy T.F. (1990). "Chemical processes in buoyant hydrothermal plumes on the East Pacific Rise near 21°N." *Geochimica et Cosmochimica Acta* **54**(7): 1911-1927.

Planquette H. and Sherrell R.M. (2012). "Sampling for particulate trace element determination using water sampling bottles: methodology and comparison to in situ pumps." *Limnology and Oceanography* **10**(5): 367-388.

Preston C.M., Harris A., Ryan J.P., Roman B., Marin R., III, Jensen S., Everlove C., Birch J., Dzenitis J.M., Pargett D., Adachi M., Turk K., Zehr J.P. and Scholin C.A. (2011). "Underwater Application of Quantitative PCR on an Ocean Mooring." *PLoS ONE* **6**(8): e22522.

Riso R.D., Le Corre P. and Chaumery C.J. (1997). "Rapid and simultaneous analysis of trace metals (Cu, Pb and Cd) in seawater by potentiometric stripping analysis." *Analytica Chimica Acta* **351**(1–3): 83-89.

Rudnicki M.D. and Elderfield H. (1993). "A chemical model of the buoyant and neutrally buoyant plume above the TAG vent field, 26 degrees N, Mid-Atlantic Ridge." *Geochimica et Cosmochimica Acta* **57**(13): 2939-2957.

Sander S.G., Koschinsky A., Massoth G., Stott M. and Hunter K.A. (2007). "Organic complexation of copper in deep-sea hydrothermal vent systems." *Environmental Chemistry* **4**(2): 81-89.

Sander S.G. and Koschinsky A. (2011). "Metal flux from hydrothermal vents increased by organic complexation." *Nature Geoscience* **4**(3): 145-150.

Sarradin P.-M., Sarrazin J., Allais A.G., Almeida D., Brandou V., Boetius A., Buffier E., Coiras E., Colaco A., Cormack A., Dentrecolas S., Desbruyeres D., Dorval P., du Buf H., Dupont J., Godfroy A., Gouillou M., Gronemann J., Hamel G., Hamon M., Hoge U., Lane D., Le Gall C., Leroux D., Legrand J., Leon P., Leveque J.P., Masson M., Olu K., Pascoal A., Sauter E., Sanfilippo L., Savino E., Sebastiao L., Santos R.S., Shillito B., Simeoni P., Schultz A., Sudreau J.P., Taylor P., Vuillemin R., Waldmann C., Wenzhöfer F. and Zal F. (2007). EXtreme ecosystem studies in the deep OCEan: Technological developments. New York, Ieee.

Sarradin P.-M., Lannuzel D., Waeles M., Crassous P., Le Bris N., Caprais J.C., Fouquet Y., Fabri M.C. and Riso R. (2008). "Dissolved and particulate metals (Fe, Zn, Cu, Cd, Pb) in two habitats from an active hydrothermal field on the EPR at 13°N." *Science of the total Environment* **392**(1): 119-129.

Sarradin P.-M., Waeles M., Bernagout S., Le Gall C., Sarrazin J. and Riso R. (2009). "Speciation of dissolved copper within an active hydrothermal edifice on the Lucky Strike vent field (MAR, 37°N)." *Science of the total environment* **407**(2): 869-878.

Shank T.M., Fornari D.J., Von Damm K.L., Lilley M.D., Haymon R.M. and Lutz R.A. (1998). "Temporal and spatial patterns of biological community development at nascent deep-sea hydrothermal vents (9°50′N, East Pacific Rise)." *Deep Sea Research II* **45**(1–3): 465-515.

Taylor C.D., Doherty K.W., Molyneaux S.J., Morrison III A.T., Billings J.D., Engstrom I.B., Pfitsch D.W. and Honjo S. (2006). "Autonomous Microbial Sampler (AMS), a device for the uncontaminated collection of multiple microbial samples from submarine hydrothermal vents and other aquatic environments." *Deep Sea Research I* **53**(5): 894-916.

Toner B.M., Fakra S.C., Manganini S.J., Santelli C.M., Marcus M.A., Moffett J.W., Rouxel O., German C.R. and Edwards K.J. (2009). "Preservation of iron(II) by carbon-rich matrices in a hydrothermal plume." *Nature Geoscience* **2**(3): 197-201.

Toner B.M., Marcus M.A., Edwards K.J., Rouxel O. and German C.R. (2012). "Measuring the form of iron in hydrothermal plume particles." *Oceanography* **25**(1): 209–212.

Trocine R.P. and Trefry J.H. (1988). "Distribution and chemistry of suspended particles from an active hydrothermal vent site on the Mid-Atlantic Ridge at 26°N." *Earth and Planetary Science Letters* **88**(1–2): 1-15.

Truitt R.E. and Weber J.H. (1979). "Trace metal ion filtration at pH 5 and 7." *Analytical Chemistry* **51**(12): 2057-2059.

Ussler W., Preston C., Tavormina P., Pargett D., Jensen S., Roman B., Marin R., Shah S.R., Girguis P.R., Birch J.M., Orphan V. and Scholin C. (2013). "Autonomous application of quantitative PCR in the deep sea: in situ surveys of aerobic methanotrophs using the Deep-sea Environmental Sample Processor." *Environmental Science & Technology* **47**(16): 9339-9346.

Von Damm K.L., Edmond J.M., Grant B., Measures C.I., Walden B. and Weiss R.F. (1985). "Chemistry of submarine hydrothermal solutions at 21°N, East Pacific Rise." *Geochimica et Cosmochimica Acta* **49**(11): 2197-2220.

Vuillemin R., Le Roux D., Dorval P., Bucas K., Sudreau J.P., Hamon M., Le Gall C. and Sarradin P.-M. (2009). "CHEMINI: A new *in situ* CHEmical MINIaturized analyzer." *Deep Sea Research I* **56**(8): 1391-1399.

Yafa C. and Farmer J.G. (2006). "A comparative study of acid-extractable and total digestion methods for the determination of inorganic elements in peat material by inductively coupled plasma-optical emission spectrometry." *Analytica Chimica Acta* **557**(1–2): 296-303.

Yeats P.A., Dalziel J.A. and Moran S.B. (1992). "A comparison of dissolved and particulate Mn and Al distributions in the Western North Atlantic." *Oceanologica Acta* **15**(6): 609-619.

Yücel M., Gartman A., Chan C.S. and Luther G.W. (2011). "Hydrothermal vents as a kinetically stable source of iron-sulphide-bearing nanoparticles to the ocean." *Nature Geoscience* **4**(6): 367-371.